REGIONAL COMPARISON OF TRENDS IN THE ARCTIC SEA ICE COVER DERIVED FROM SATELLITE PASSIVE MICROWAVE DATA SETS

Yuta TOCHIGI, Kohei CHO, Koki NISHIURA, Yutaka TONEGAWA
Tokai University
2-28-4 Tomigaya. Shibuya -ku, Tokyo 151-0063 Japan
Tel: (81)-3-3481-0611 Fax: (81)-3-3481-0610
E-mail: cho@yoyogi.ycc.u-tokai.ac.jp

KEY WORDS: Northern hemisphere, SSM/I, thin sea ice

ABSTRACT: The previous studies of passive microwave satellite observations suggested the decreasing trend of the Arctic sea ice extent. In this study, authors have calculated the averaged sea ice area of the each sea ice region in the northern hemisphere, and calculated the sea ice area shrinking speed of each sea ice region during 1988 to 2006 from SSM/I data sets provided from NSIDC. The result suggested that the fastest sea ice shrinking speed was of the Gulf of St. Lawrence, and the second was of the sea ice region consists of Baffin Bay, Davis Strait, and Labrador Sea. The authors have extracted "presumed thin sea ice area" of those sea ice regions by using the sea ice concentration difference between NASA Team and Bootstrap algorithms. Even though the trend of total sea ice area were decreasing, the "presumed thin sea ice area" during February and March were rather stable in both sea ice regions during 1988 to 2006.

1. INTRODUCTION

The passive microwave sensors on board satellites allow us to monitor the distribution of sea ice on global scale. The previous studies of passive microwave satellite observations suggested the decreasing trend of the Arctic sea ice extent (Cavarieri et al. 2003, Fetterer et al. 2008, Comiso et al. 2008). The sea ice reduction trend described in the recent IPCC report (IPCC, 2007) is mainly relying on the results of the passive microwave satellite observations. Usually, sea ice concentrations derived from satellite passive microwave sensor data are used to estimate the trend of sea ice distribution. There are mainly two ways to calculate the sea ice distribution. One is "sea ice extent" and the other is "sea ice area". The sea ice extent is defined as a measurement of the area of ocean where there is at least more than certain percentage (for example 15%) of ice concentration. The sea ice area is calculated by summing up the sea ice area of each pixel of passive microwave sensor data. The sea ice area of each pixel is calculated from the ice concentration of each pixel. From the definition, sea ice extent is always larger than sea ice area. Since sea ice concentration calculation more or less differs between algorithms, calculation of sea ice extent is considered to be more stable and algorithm independent than calculation of sea ice area.

There are mainly two algorithms which are widely used for calculating sea ice concentration from satellite passive microwave sensor data. One is NASA Team Algorithm (Cavalieri et al., 1984, 1992), and the other is Bootstrap Algorithm (Comiso 1986, 1995). The comparison of the two algorithms (Comiso, Cavarieli et al.1997) showed small disagreements in the central Arctic in winter but larger disagreement in the seasonal region and in summer mainly caused by temperature effects and emissivity effects. The study in the Arctic peripheral seas suggested that NASA Team Algorithm is likely to underestimate concentration compared with Bootstrap Algorithm (Meier 2005). In our study, the authors have decided to used Bootstrap algorithm for calculating sea ice area of each sea ice region in the northern hemisphere, and compared the trend.

2. SEA ICE REGIONS AND ANALYZED DATA

The nine sea ice regions of the northern hemisphere were analyzed in this study. Figure 1 shows the location map of the sea ice regions. The identification of the regions is following those of the National Snow & Ice Data Center (NSIDC, 2008). The brightness temperature data, sea ice concentration data, and total sea ice area data derived from passive microwave sensor SSM/I observation from 1988 to 2006 were used for the analysis. In order to avoid sensor sensitivity differences, only SSM/I data was used as passive microwave sensor data source. All the data were provided from NSIDC. In this study, Bootstrap algorithm was mainly use for calculating sea ice concentration and sea ice area from SSM/I data. NASA Team algorithm was also used for extracting "presumed thin sea ice area".

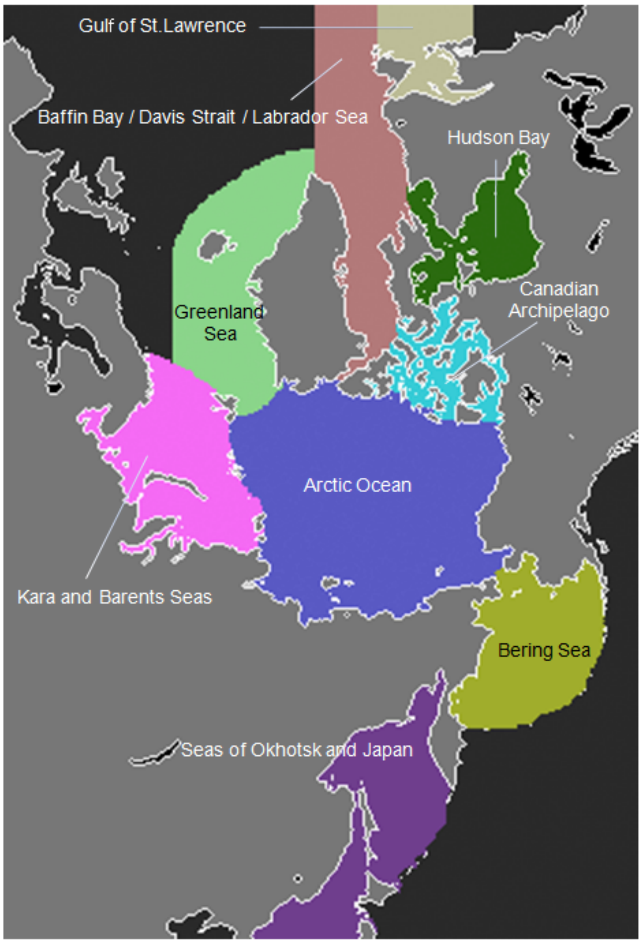

Figure 1. Identification of the sea ice regions analyzed in this study.(After NSIDC, 2008)

3. METHODOLOGY

3.1 Sea ice area trend analysis

In order to evaluate the interannual trend of sea ice in the northern hemisphere, we produced several graphs from SSM/I data sets provided from NSIDC. Average sea ice area of each sea ice region was calculated to evaluate the scale of each sea ice region. By dividing the sea ice area trend (unit: km^2/year) with averaged sea ice area (unit: km^2), we evaluated the shrinking speed of each sea ice region.

3.2 Presumed thin sea ice area analysis

It is quite important to evaluate not only the trend of sea ice area but also the trend of thin sea ice area. Cho et al. (2007) have compared the SSM/I sea ice concentration image with MODIS image in the Sea of Okhotsk, and suggested the possibility of extracting thin sea ice area by using the sea ice concentration difference between Bootstrap and NASA Team algorithms. Usually, in microwave region, the existence of water around and over thin sea ice may reduce the brightness temperature more in horizontal (H) polarization than in vertical (V) polarization. Since Bootstrap algorithm uses only V polarization data of the passive microwave sensors and NASA Team algorithm uses both V & H polarization data, NASA Team algorithm is more likely to calculate lower sea ice concentration than Bootstrap algorithm in thin sea ice area. In this study, we used the sea ice concentration difference between Bootstrap and NASA Team algorithms for extracting "presumed thin sea ice area". The "presumed thin sea ice area" is not equal to thin sea ice area. However, it may more or less reflect the distribution of thin sea ice area. In order to avoid the sea ice surface melting effect during the summer, we calculated the trend of "presumed thin sea ice area" only during February and March from 1988 to 2006 for the Baffin Bay and the Gulf of St. Lawrence.

4. INTER ANNUAL TREND OF SEA ICE AREA

4.1 Total Arctic

Figure 2 shows the trend in total Arctic sea ice extent and area derived with the Bootstrap algorithm. The trend of sea ice area is approx. –69,000km^2 per year. The trend difference between sea ice area and sea ice extent is rather small. Thus, sea ice area is mainly used for the trend analysis in this study.

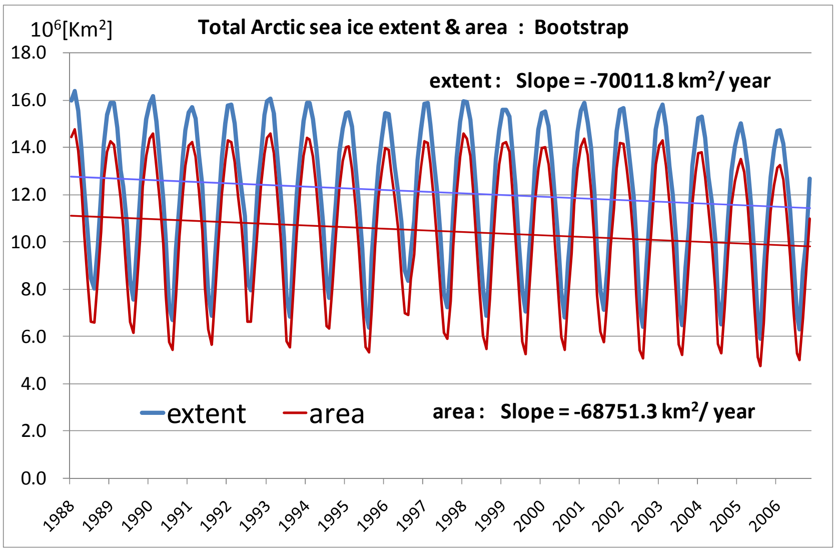

Figure 2. Total Arctic sea ice extent and area derived from SSMI (Data source: NSIDC)

4.2 Sea ice region comparison

In order to evaluate the percentages of the sea ice area of each sea ice region in the northern hemisphere, the averaged sea ice area per year of each sea ice region was calculated from 1988 to 2006. Figure 3 shows the circle graph of the percentages of averaged sea ice area of each sea ice region in the northern hemisphere.

From Figure 3(a), it is clear that approx. 60% of the sea ice area in northern hemisphere is of the Arctic Ocean, and none of the other sea ice region have more than 11% of the total sea ice area of the northern hemisphere. From Figure 3(b), we can say that the most contributing sea ice region for the reduction of sea ice area in the northern hemisphere is the Baffin Bay.

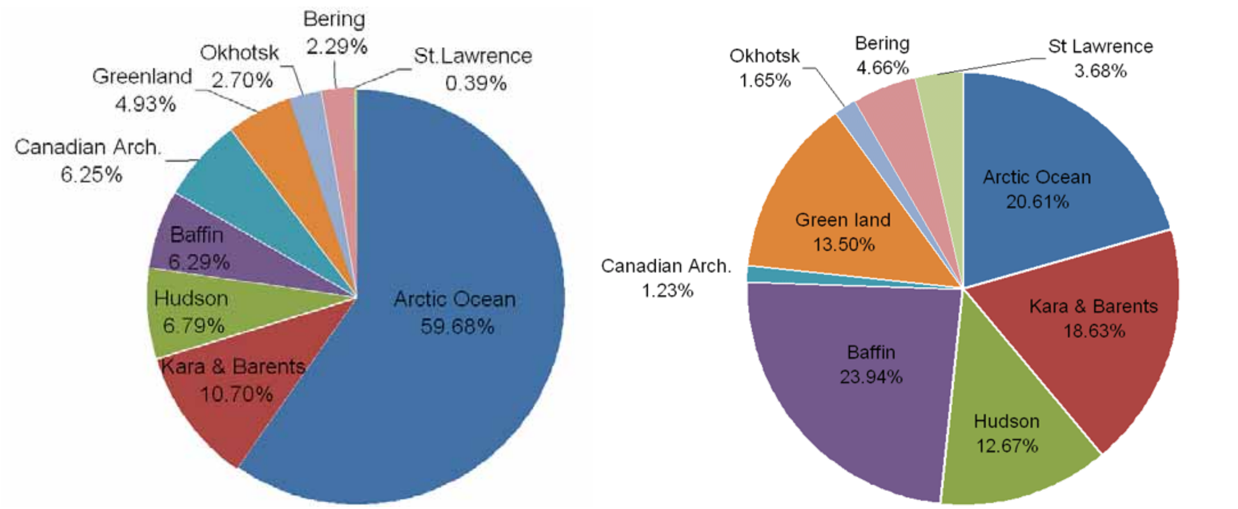

(a) Averaged sea ice area **(b) Averaged sea ice area reduction rate**

Figure 3. Percentages of averaged sea ice area and averaged sea ice area reduction per year of each sea ice region in the northern hemisphere from 1988 to 2006.

Usually, the trend of sea ice area or sea ice extent is used for evaluating sea ice reduction speed of sea ice regions. In this study, we have divided the trend of sea ice area by the averaged sea ice area of each sea ice region to calculate the shrinking speed (% per year) of each sea ice region. The shrinking speed reflects how many percentage of sea ice area within the sea ice region is shrinking per year. The results are shown on Figure 4. The left bar shows the averaged sea ice area and the right bar shows the averaged sea ice shrinking speed of each sea ice region. From this figure, it is clear that the sea ice shrinking speed of St Lawrence, which is the smallest sea ice region in the northern hemisphere, is the fastest. Also, we can see that the shrinking speed of Baffin Bay is the second.

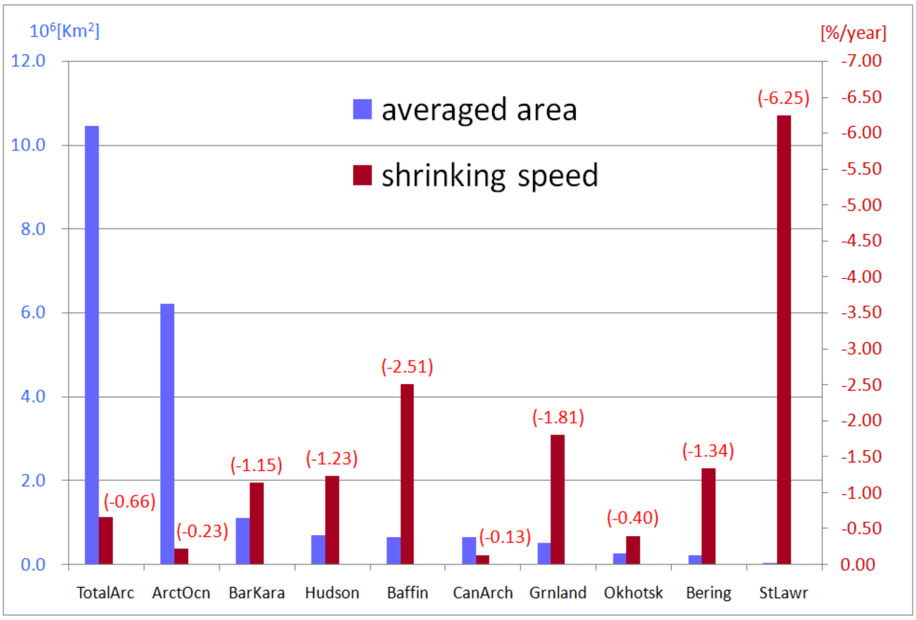

Figure 4. Averaged sea ice area and shrinking speed of each sea ice region in northern hemisphere.

4.3 Trend analysis of Baffin Bay and Gulf of St. Lawrence

Considering the fast shrinking speed of the Gulf of St. Lawrence and Baffin Bay, we have analyzed the two sea ice regions in details. It should be noted that sea ice region “Baffin Bay” in this study includes Davis Strait and Labrador Sea as shown on Figure 1.

Figure 5(a) shows the sea ice concentration image of the Baffin Bay. The Bootstrap ice concentration image was colored in red and the NASA Team ice concentration image was colored in blue+green. If the both algorithms calculate same ice concentration, the area appears in white or gray. If the sea ice concentration was calculated more in Bootstrap, the area appears in red. Figure 5(b) shows the zoom up of the image and Figure 5(d) shows the MODIS image of the same area. The MODIS image is color composite of Band 1(colored in blue and red), Band 2(colored in green) with 250m IFOV. By comparing Figure 5(b) and (d), we have decided that if Bootstrap sea ice concentration was higher than 80% and Bootstrap minus NASA Team sea ice concentration was higher than 30%, we define the area as “presumed thin sea ice area“. The green area on Figure 5(c) show the “presumed thin sea ice area” extracted with this condition. By using this condition, we have calculated the “presumed thin sea ice area” of the Baffin Bay and the Gulf of St. Lawrence from daily SSM/I sea ice concentration data of February and March from 1988 to 2006. Figure 6(a) and (b) show the trend of two months averaged sea ice area and “presumed thin sea ice area” of the both sea ice regions.

When we see the trend of total sea ice area, both regions show similar reduction trend. On the other hand, the trends of percentage of “presumed thin sea ice area” within each region were quite stable. The percentages of “presumed thin sea ice area” were constantly about 3% in the Baffin Bay and about 15% in the Gulf of St. Lawrence. This suggests that even though the trends of sea ice area of the both regions are reducing, the trend of the percentages of thin sea ice area within both regions may not have been increasing so far.

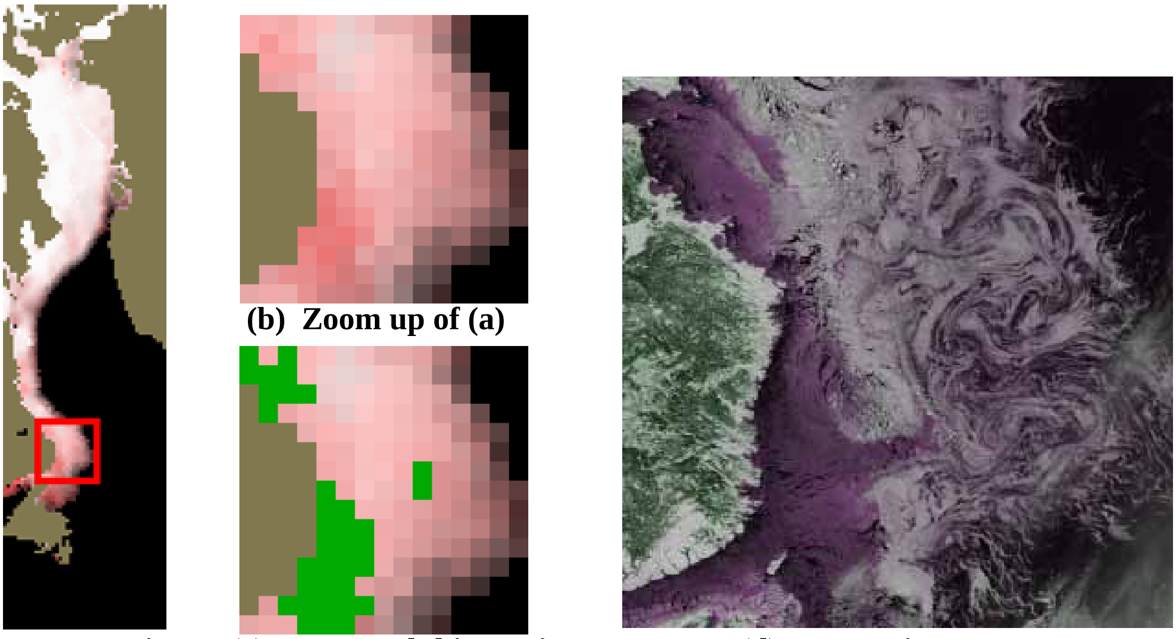

(a) SSM/I sea ice concentration image (c)"presumed thin sea ice area" (green) (d) MODIS image

Figure 5. Extraction of "presumed thin sea ice area" in the Baffin Bay (Feb. 22, 2006)

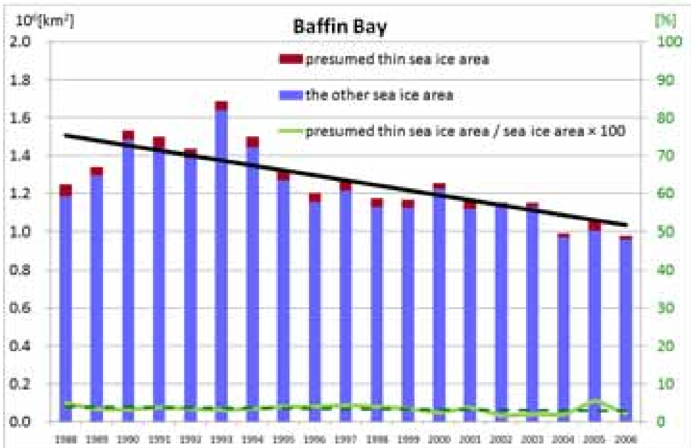

(a) Baffin Bay

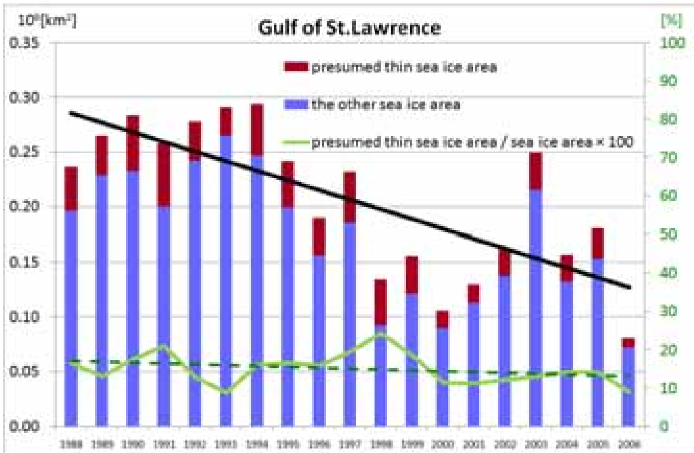

(b) Gulf of St. Lawrence

Figure 6. Trend of two months averaged sea ice area and percentage of "presumed thin sea ice area" derived from SSM/I data of February and March, 1988 to 2006.

5. CONCLUSION

In this study, authors have calculated the averaged sea ice area of the each sea ice region in the northern hemisphere, and calculated the sea ice area shrinking speed of each sea ice region from SSM/I data sets provided from NSIDC. The result suggested that the fastest sea ice shrinking speed was of the Gulf of St. Lawrence, and the second was of the Baffin Bay (including Davis Strait, and Labrador Sea). In order to evaluate the sea ice trend of those sea ice regions in details, the authors have extracted “presumed thin sea ice area” of those sea ice regions by using the sea ice concentration difference between NASA Team and Bootstrap algorithms. When we see the trend of total sea ice area, both regions show similar reduction trend. On the other hand, the trends of percentage of “presumed thin sea ice area” within each region were quite stable. The percentages of “presumed thin sea ice area” were constantly about 3% in the Baffin Bay and about 15% in the Gulf of St. Lawrence. This suggests that even though the trends of sea ice area of the both regions are reducing, the trend of percentages of thin sea ice area may not have been increasing so far. However, it should be noted that the “presumed-thin sea ice area” in this study is not equal to thin sea ice area. The further study is needed to improve the methodology for extracting thin sea ice area from passive microwave sensor data more precisely.

ACKNOWLIDGEMENT

This study has been supported by Tokai University Frontier Project. The SSM/I sea ice data sets used in this study were provided from NSIDC. The authors would like to thank Tokai University and NSIDC for their support.

References

Cavalieri, D. J., et al., 30-Year satellite record reveals contrasting Arctic and Antarctic decadal sea ice variability, 2003, Geophysical Research Letters, Vol.30, No.18, CRY4-1,2.

Fetterer, F., and K. Knowles. 2002, updated 2008. Sea ice index. Boulder, CO: National Snow and Ice Data Center. Digital media.

Comiso, J. C. and F. Nishio, 2008, Trends in the sea ice cover using enhanced and compatible AMSR-E, SSM/I, and SSMR data, JGR, Vol.113, C02S07, doi:10.1029/2007JC004257.

IPCC, 2007: Summary for Policymakers. In: Climate Change 2007: The Physical Science Basis. Contribution of Working Group I to the Fourth Assessment Report of the Intergovernmental Panel on Climate Change [Solomon, S., D. Qin, et al.]. Cambridge University Press, Cambridge, United Kingdom and New York, NY, USA.

Cavalieri, D. J. and P. Gloersen, 1984, “Determination of sea ice parameters with the NIMBUS 7 SMMR”, J. Geophys. Res., Vol.89, pp.5355-5369.

Cavalieri, D. J., 1992, “NASA Sea Ice Validation Program for the Defense Meteorological Satellite Program Special Sensor Microwave Imager: Final Report”, NASA Technical Memorandum 104559, Maryland, NASA Center for AeroSpace Information.

Comiso, J. C., 1986, “Characteristics of Arctic winter sea ice from satellite multispectral microwave observations”, J. Geophys. Res., Vol.91, pp.975-994.

Comiso, J. C., 1995, “SSM/I Sea Ice Concentrations Using the Bootstrap Algorithm”, NASA Reference Publication 1380, Maryland, NASA Center for AeroSpace Information.

Comiso J.C., et al., 1997, Passive Microwave Algorithms for Sea Ice Concentration: A Comparison of Two Techniques, Remote Sensing of Environment, Vol.60, pp.357-384

Meier, W. N. 2005. Comparison of passive microwave retrievals with AVHRR imagery in arctic peripheral seas. IEEE Transactions on Geoscience and Remote Sensing 43 (6): 1324-1337.

http://nsidc.org/data/docs/daac/nsidc0051_gsfc_seaice.gd.html, 2008.

CHO K., et al., Comparison of passive microwave sea ice algorithms for detecting the trend of global warming, 2007, Proc. of the 28th Asian Conference on Remote Sensing, PL2, pp.1-6.